ASSESSMENT OF LOAD DEPENDENT FRICTION COEFFICIENTS AND THEIR INFLUENCE ON SPUR GEARS EFFICIENCY

A. Diez-Ibarbia · **A. Fernandez-Del-Rincon** · **P. Garcia** ·
A. De-Juan · **M. Iglesias** · **F. Viadero**

Abstract Traditional procedures to calculate efficiency on gear transmissions generally consider sliding friction as the only dissipative effect, and what is more, they are based on the usage of constant friction coefficients. Although this approach gives acceptable efficiency values depending on the transmission application, the utilisation of a variable friction coefficient provides more reliable results of the friction behavior. Within this framework, the influence of the choice of the friction coefficient on the efficiency of shifted spur gears is assessed in this study. The Niemann′s friction coefficient formulation, which is constant and commonly applied to traditional approaches, was implemented in this proposal, in order to compare it with two hybrid formulations, which are based on Elastohydrodynamic Lubrication fundamentals and capable to reproduce the friction coefficient in dry contact, boundary, mixed and fluid film conditions of lubrication. These friction coefficient formulations are dependent on the load applied in the conjunction, therefore an enhanced load sharing allows for a better modelling of sliding friction, not only because it depends directly on the normal forces, but due to the friction coefficient load dependence. In this regard, the Load Contact Model previously developed by the authors, which considers the deflections of the adjacent teeth and shifting profile to calculate the load sharing and the friction coefficient, is used, allowing for efficiency values with a high level of accuracy. The efficiency results obtained when hybrid formulations are implemented provides lower values than those determined including Niemann′s formulation. Furthermore, there is a shifting profile which makes optimal the efficiency. This shift factor depends on the implemented friction coefficient formulation, concluding the remarkable importance of the friction coefficient choice.

1 Introduction

Energy saving has been one of the major concerns in Industry for the last decades, since a cost reduction has been always pursued. In this regard, energy saving and efficiency in gear transmissions have been studied because of their wide use in lots of sectors such as automotive [27–30], aviation [6] and energy ones [38]. Furthermore, due to the new stricter environmental regulations [31], this issue does not only concern economical profits but people health. Within this framework, a large number of experimental and numerical efficiency analysis has been performed in the gearboxes field [11,14,19,34–36,40,41], deducing that several are the causes, in gear transmissions, which produce a reduction in the system efficiency [14,19,34,40]. Most of these causes can be characterized by their load dependence [14,19,34]. Among the load-dependent losses, the ones due to rolling and sliding friction forces among gear teeth have a major role regarding the efficiency. Whilst, among the non load-dependent losses, the ones due to the fluid motion (lubricant, coolant or/and air) are the most significant [14,21,23–25,42]. The power losses due to the fluid motion mainly depend on the speed rotation. Despite the pinion speed rotation, whose highest value was 6.000 rpm in this study, could be significant, the assumption of not considering non load-dependent losses was done. Furthermore,

A. Diez-Ibarbia
Department of Structural and Mechanical Engineering. ETSIIT University of Cantabria
Avda. de los Castros s/n. 39005 Santander. Spain
Tel.: +34-942201478
Fax.: +34-942201853
E-mail: diezia@unican.es

due to the insignificant contribution on the efficiency of the rolling friction effects in the study conditions [2,34,35], the sliding friction effect became essential, hereinafter called friction.

Since the friction forces are generally formulated by a Coulomb's model, the efficiency is mainly conditioned by three factors; Sliding Velocity (SV), Friction Coefficient (FC) and Load Sharing (LS) [19]. Traditional approaches of efficiency calculation used to consider analytical curves of load sharing and friction coefficient (constant along the mesh cycle) in order to simplify its determination [19,34]. These approximations lead to an error which in some applications is acceptable, nevertheless, in others it is necessary the use of a methodology which takes into account the power losses accurately, in other words, a methodology which calculates both the load sharing and friction coefficient as close as possible to their real behaviour. Regarding this, the Load Contact Model (LCM) previously developed by the authors, which is based on the Hertzian theory [15–17], was used in order to assess the added value of using an accurate load calculation approach. This LCM was developed to model spur gear transmissions in presence of defects, in order to prognosticate the dynamic response of these kinds of systems (predictive maintenance) [15–17]. It was extended to planetary gears, modelling in this way both internal and external contacts [20], focusing on the load sharing formulation. Furthermore, the need of formulations capable to reproduce the friction coefficient accurately in every lubrication conditions (dry contact, boundary, mixed and fluid film lubrication) makes of great interest the fact of implementing several formulations to compare the impact of considering a simple or an advanced friction coefficient [1,33]. In this work, the well-known Niemann formulation, which is commonly used in traditional procedures of efficiency determination, and two hybrid formulations were implemented. These hybrid formulations require a friction coefficient experimentally measured in dry contact conditions, a friction coefficient in fluid film conditions of lubrication (Xu *et al.* is utilised) and a weighting function (developed by Castro *et al.* and Zhu *et al.*). With these two accurate formulations, the dissimilarities with the acceptable Niemann friction coefficient related to efficiency and friction coefficient values can be established. From the above, it is inferred the importance of utilising accurate formulations of the contact forces and friction coefficients along the mesh cycle to determine the efficiency. This is the reason why, in this work, the efficiency results implementing the Niemann's FC, which were presented in previous works [10], are used as reference to show the benefits of employing an advanced friction coefficient formulation, correlating in this manner the obtained friction and efficiency results with ISO/TC 60 standard [10].

Another aspect assessed in this work is the profile shifting, which is widely employed in several sectors of the Industry to balance the durability of gear transmissions with a gear ratio different from the unity. This kind of transmissions presents the problematic that the pinion reaches the end of its useful life long before the driven wheel. Thus, with a positive shifting in the pinion, its durability is increased, performing the opposite procedure in the driven gear. This profile shifting has an impact on all the parameters that affect the efficiency (sliding velocity, friction coefficient and load sharing), thus, determining this impact is a question of great interest. In this study, it was assumed that shift factors of the pinion and gear were equal in absolute value, but with opposite signs ($x_1+x_2= 0$ was constrained for the whole study), in order not to modify the working distance of the transmission. So as to achieve this goal, the inclusion of gear profile shifting as a LCM feature was compulsory and therefore developed beforehand [15–17]. Furthermore, the methodology presented in [9,10] was utilized to calculate the efficiency.

The novelty with respect previous works is the incorporation of a friction coefficient formulation capable to reproduce the behavior in the conjunction under Elastohydrodynamic lubrication, regardless the conditions of the contact. This was done in order to comprehend what is the advantage of using an enhanced friction coefficient formulation with respect to a constant one in the efficiency calculation. This is the reason why, in this work, a comparison of the efficiency results implementing this enhanced friction coefficient, with those obtained using Niemann's friction coefficient [10], is performed . The strength of this proposal is the calculation of the efficiency using a procedure which considers an advanced Load Contact Model to obtain the load sharing and the friction coefficient. With respect to traditional approaches [19], which approximate these two parameters as analytical curves, the utilised procedure calculates numerically the forces in the conjunction by reaching the equilibrium of the system. Furthermore, the load sharing affects directly the power losses due to the fact that sliding friction is implemented as a Coulomb's model, but not only that, it also has a major impact on the friction coefficient determination because its formulation and the lubrication regime depend on the applied load. As the utilised load sharing has a high level of accuracy, since the profile shifting, the deflections of the adjacent teeth and the torque level are taken into account in its calculation, the proposed procedure presents a double advantage with respect to other approaches.

Since this work is focused on studying the friction coefficient impact on the efficiency, Section 2 shows the different formulations of FC considered. Subsequently, its role on the efficiency calculation is presented in Section 3. Section 4 provides the characteristics of the transmission example of application and the layout

of the shifting case studies considered. In Section 5, the results of efficiency are shown, whilst the conclusions of the work are disclosed in Section 6.

2 Friction coefficient models and applied fundamentals of lubrication

To avoid the power losses due to friction, metal to metal contact and overheating in the teeth, lubricants are extensively used in gear transmissions to cool and lubricate the conjunction. Depending on the transmitted load from the pinion to the driven gear in functioning, rheological and material properties, four different regimes of lubrication are usually distinguished: Viscous elastic also called EHL, viscous rigid, iso-viscous elastic and iso-viscous rigid known as Hydrodynamic Lubrication (HL) [12]. To identify among regimes of lubrication, some parameters have been developed, being two of the most commonly used the Greenwood parameters (G_e and G_v) and the Stribeck's one (λ) [7,8].

In this work, first, Greenwood parameters were utilized (equation 1) to assure that the transmission was on EHL regime.

$$G_e = \frac{(2W)^{8/3}}{(2U)^2} \quad \text{and} \quad G_v = \frac{GW^3}{U^2} \tag{1}$$

Where W, U and G were non-dimensional parameters related respectively to the load, rheological and material properties as shown in equation 2.

$$W = \frac{q}{2 \cdot 10^9 E_{eq}\rho_{eq}}, \quad U = \frac{2V_e\eta_{oil}}{2 \cdot 10^9 E_{eq}\rho_{eq}} \quad and \quad G = 2\alpha E_{eq} \tag{2}$$

Being E_{eq} the Young modulus, η_{oil} the oil dynamic viscosity, V_e the fluid entraining velocity, q the load per unit of length, ρ_{eq} the equivalent radius of curvature and α the viscosity-pressure coefficient.

Then, once the regime of lubrication was defined, the conditions of the EHL were determined by the Stribeck parameter. This value is generally defined as the relation between the fluid film thickness and the roughness of the teeth profile ($\lambda(\theta) = h_0(\theta)/R_a$). This parameter has some limitations since only two lubricant regimes can be identified (EHL and HL). It is usually considered that the boundary of this two regimes of lubrication takes place when λ is about 10. Nevertheless, it allows to distinguish in which EHL conditions the contact is [4,7]. In other words, if the contact conditions are Boundary (BL), Mixed (ML) or Fluid film Lubrication (FL). The boundaries among EHL conditions can be seen in Figure 2.

Stribeck parameter depends directly on the film thickness calculation (h_0). Hereof, the Dowson and Hamrock formulation for line contacts was implemented (equation 3) [18,22].

$$h_0 = \rho_{eq}2.922W^{-0.166}U^{0.692}G^{0.47} \tag{3}$$

In this proposal, a Coulomb's model was utilised to implement friction forces. Since the variation on friction coefficient is to be analysed, three different formulations were used: (i) Niemann's proposal [3,19,26,32] and two hybrid formulations derived from (ii) Castro *et al.* weighting function and [5,13] (ii) Zhu *et al.* weighting function [13,43].

2.1 Niemann's formulation

The first FC utilized is the widely used Niemann's formulation [3,19,26,32]. This formulation, which is constant along the mesh cycle, depends on the contact force, speed and geometrical and rheological parameters. It is extensively used in analytical expressions since it is an average value and make easier solving the power losses due to friction (equation 10).

$$\mu = 0.048\left(\frac{\frac{F_{Nmax}}{b}}{V_{\Sigma C}\rho_c}\right)^{0.2} \eta_{oil}^{-0.05}R_a^{0.25}X_L \rightarrow \begin{cases} V_{\Sigma C} = 2V_t sin(\varphi) \\ X_L = \frac{1}{\left(\frac{F_{Nmax}}{b}\right)^{0.0651}} \end{cases} \tag{4}$$

ρ_c is the equivalent curvature radius in the pitch point, F_{Nmax} the maximum contact force, V_t the tangential speed in the pitch point, b the gear width, φ the pressure angle and R_a the mean roughness of the teeth profile.

2.2 Hybrid formulations

With the aim of obtaining a valid friction coefficient in all the lubrication regimes and conditions, a hybrid formulation was developed [5, 13, 43]. This formulation integrates, by means of a weighting function ($f_\lambda(\theta)$), a friction coefficient in dry contact conditions (μ^{DC}) and another in EHL fluid film conditions ($\mu^{FL}(\theta)$) as shown in equation 5. With this weighting function, a friction coefficient, which is suitable in dry contact conditions, boundary, mixed and fluid film lubrication, is obtained.

$$\mu^{ML}(\theta) = \mu^{FL}(\theta) f_\lambda(\theta) + \mu^{DC}(1 - f_\lambda(\theta)) \tag{5}$$

Regarding the weighting function, two of the most generally used in the literature has been implemented [43]; Castro *et al.* (equation 6) and Zhu *et al.* (equation 7), which are giving the name to the friction coefficient in this study. These functions are dependent on the Stribeck parameter.

$$f_\lambda(\theta) = 0.82\lambda(\theta)^{0.28} \tag{6}$$

$$f_\lambda(\theta) = \frac{1.21\lambda(\theta)^{0.64}}{1 + 0.37\lambda(\theta)^{1.26}} \tag{7}$$

With respect to the friction coefficient in dry contact conditions, an experimental measurement has been employed for the steel alloy considered ($\mu^{DC} = 0.227098$) [7].

Furthermore, regarding the friction coefficient in EHL fluid film conditions, the formulation used in the study is the developed by Xu *et al.* [40, 41]. This variable friction coefficient was obtained by making a regression analysis of experimental tests in the specified conditions of lubrication.

$$\mu^{FL}(\theta) = e^{f(SR, P_h, \eta_{oil}, R_a)} P_h^{b_2} |SR|^{b_3} V_e^{b_6} \eta_{oil}^{b_7} \rho_{eq}^{b_8} \tag{8}$$

Where P_h is the Hertzian pressure in the conjunction (GPa) and, SR a non-dimensional parameter which is the ratio between sliding and entraining velocity. All these parameters vary along the contact depending on the angular position.

$$f(SR, P_h, \eta_{oil}, R_a) = b_1 + b_4 |SR| P_h \log \eta_{oil} + b_5 e^{-|SR| P_h \log \eta_{oil}} + b_9 e^{R_a} \tag{9}$$

The value of the constants b_j is $b_j = [-8.916465, 1.03303, 1.036077, -0.354068, 2.812084, -0.100601, 0.752755, -0.390958, 0.620305]$.

In this work, the considered lubricant in the conjunction was 75W90 mineral oil, which properties at the working temperature are presented in 1 and are constraint to be constant during the whole meshing cycle.

Table 1: Lubricant parameters

75W90 mineral oil at 373^oK	
Viscosity-pressure coefficient (α)	Dynamic viscosity (η_{oil})
22 GPa^{-1}	10.6 $mPas$

As example, Figure 1 shows the differences among friction coefficients in the same operating conditions (159 Nm and 1500 rpm). As something remarkable, it can be seen the deviation among the FC formulations, which use weighting function (Castro and Zhu FC), and the Xu FC one, which considers that the contact is under fluid film lubrication.

Furthermore, Figure 2 shows the Stribeck curve in the five considered operating conditions (Table 2), with the aim of having an overview of the lubrication regimes in the conjunction. It can be established the need of including the weighting function since there are contacts which occur under mixed lubrication conditions (operating conditions 1, 3 and 4) and not only under fluid film lubrication as Xu *et al.* FC simulates. In this regard, the deviation between the weighting function of Castro *et al.* and Zhu *et al.* can be appreciated in detail in Figure2(b) (Mixed Lubrication region).
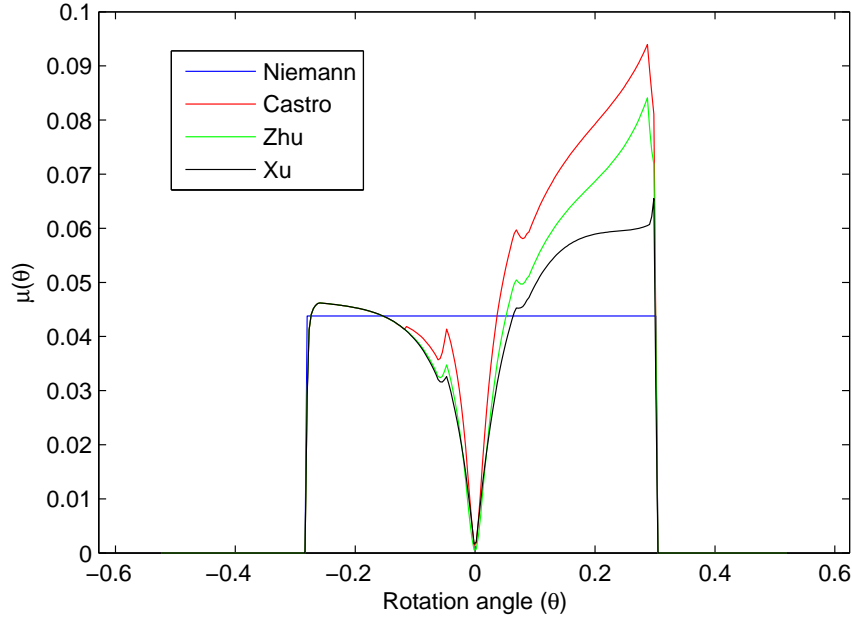
Fig. 1: Friction coefficient formulations example (159 Nm and 1500 rpm)

3 Basis of the efficiency calculation

Since an efficiency calculation methodology was presented in previous works [10], in this section, only the parameter necessary for the comprehension of the study are presented. Mechanical efficiency is dependant on the system power losses (P_{loss}) and, in consequence of considering only frictional effects, these power losses were defined as:

$$P_{loss} = \frac{F_{tmax}}{cos\left(\varphi\right)} \frac{V}{p_{et}} \int_{\theta_A}^{\theta_E} IPLd\theta \Rightarrow IPL = \frac{\mu(\theta)F_N\left(\theta\right)V_s\left(\theta\right)}{F_{Nmax}V} \tag{10}$$

Where $V_s\left(\theta\right)$ is the sliding velocity, $\mu\left(\theta\right)$ is the friction coefficient and $F_N\left(\theta\right)$ is the normal load. All these parameters are variable with the angular position (θ). Moreover, θ_A and θ_E are the angular positions corresponding to the beginning and end of the mesh cycle, F_{tmax} the maximum tangential force, V the pitch line velocity along the mesh cycle and p_{et} the transverse pitch.

On the right hand side of the equation 10, it can be appreciated the terms which are decisive on the power loss value. In order to make an evaluation of the efficiency value, it was useful to define a non-dimensional factor which was called Instantaneous Power Loss (IPL) factor [10]. It shows where the power losses takes place and also which parameter, among the ones which influence on the efficiency, has a major contribution.

Three parameters are appreciated to affect IPL factor, the friction coefficient, the Sliding Velocity Factor ($SVfactor= V_s\left(\theta\right)/V$) and the Load Sharing Ratio ($LSR= F_N\left(\theta\right)/F_{Nmax}$). The $SVfactor$ is directly calculated since the pitch point was predefined to be in the tangent of both pitch circumferences. Thus, the analysis of the other two parameters and their variability is crucial in the efficiency calculation.

The LS used is obtained from the LCM, which was presented in [16,17,39]. This calculation follows the Vedmar *et al.* procedure [37], in which the elastic deformations due to the contact in the conjunction are divided into two main contributions: i) global and ii) local deflections. In the utilised model, the global deformations are accomplished using the FE theory, and what is more, the model employs the Hertzian contact basis to calculate the local deformations. The fundamentals of both models are detailed in [15–17]. Moreover, since a quasi-static analysis is performed, the contact forces are obtained by reaching the torque equilibrium in each angular position. This is achieved by an iterative process which calculates the torque created by these forces and equalise them to the resistive torque applied to the system. Depending on the forces considered (normal contact forces, sliding and rolling friction forces, forces due to churning and windage effects and so on), this equilibrium changes and therefore the LS. In this work, the equilibrium is reached taking into account the normal contact forces as well as the forces due to friction. This fact influences
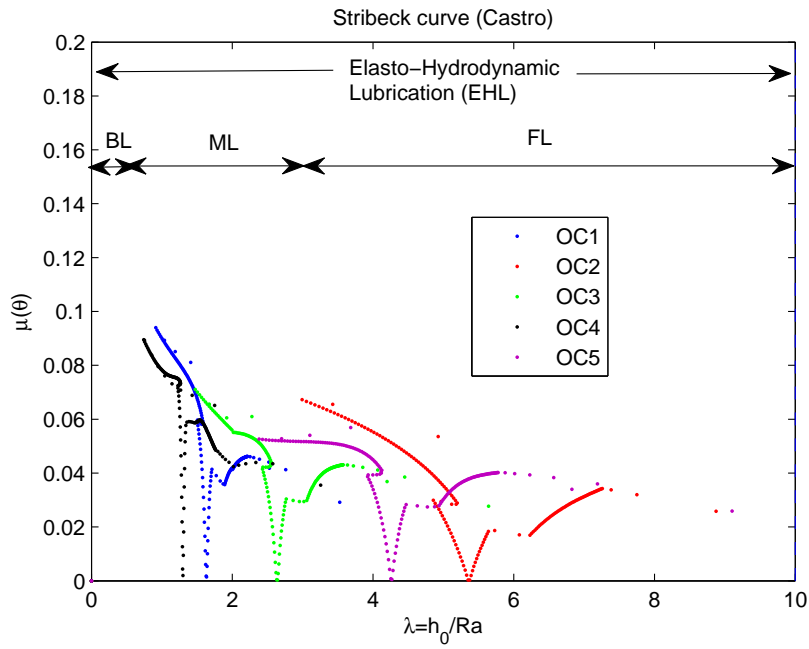
(a) Stribeck curve in the five operating conditions (see Table 2)
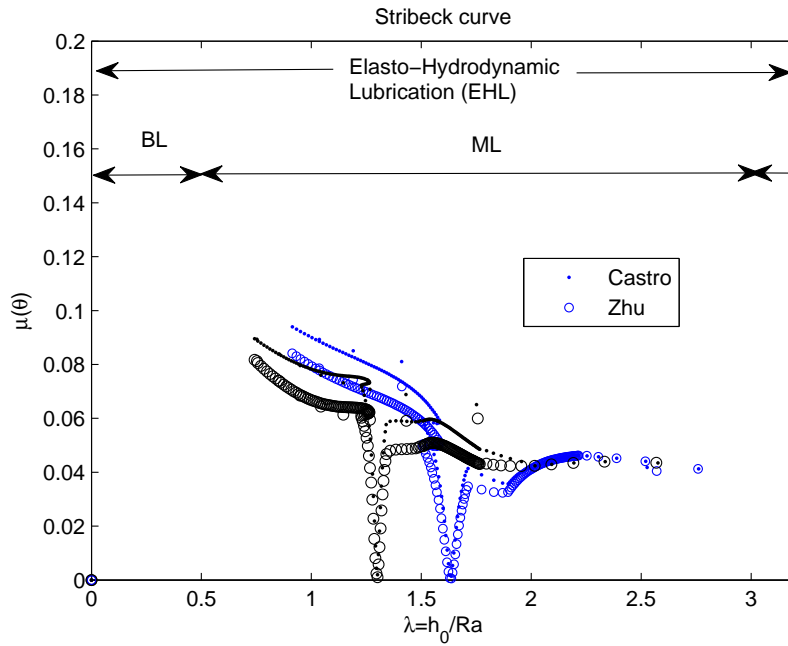
(b) Stribeck curve in the mixed lubrication region

Fig. 2: Overview of the lubrication regimes by means of the Stribeck curves a) in the five operating conditions (see Table 2) with no shifting and b) showing dispersion between weighting functions in mixed lubrication

the LS distribution, as appreciated in Figure 3. This difference is mainly noticed in the single contact region and depends on the implemented friction coefficient formulation. This variation occurs because of the friction forces, which change of direction in the pitch point region. Before the pitch point, the friction force torque is opposed to the contact forces torque, whilst, after the pitch point, it is in favour.

The FC formulations and their role were presented in Section 2. As they are highly influenced by the applied force in the conjunction, the LS distribution affects the efficiency calculation twice, directly and in

the FC determination. Thus, it is crucial to have a good LCM which reproduces accurately the transmission behavior.
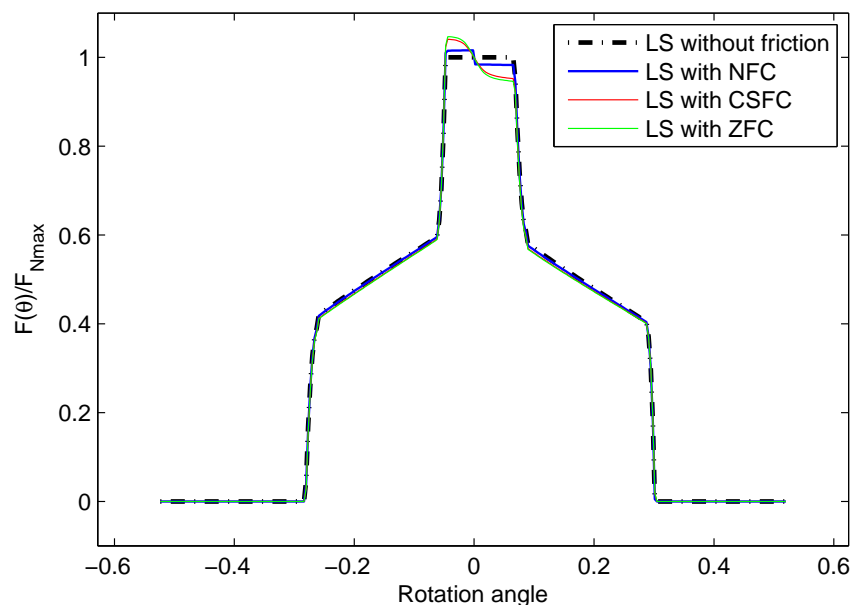

Fig. 3: Load Sharing formulations: example with no shifting profile (159 Nm and 1500 rpm), when no friction coefficient is implemented, with Niemann's (NFC), with Castro's (CSFC) and with Zhu's (ZFC) friction coefficients

4 Spur gear transmission example of application

The spur gear transmission parameters and operating conditions used in this work are presented in Tables 2 and 3. The transmission example of application is the same as in previous works [10], since the results obtained with Niemman′s FC were the reference point to extend the study to new FC formulations.

Table 2: Transmission parameters

Main parameters			
Number of pinion teeth	18	Module	3
Number of gear teeth	36	Pressure angle	20º
Mean Roughness	0.8 μm	Face width	26.7 mm

Table 3: Operating and lubrication conditions of the transmission

Operating conditions	Power (kW)	Torque (Nm)	Speed (rpm)	Lubrication Conditions
OC1	25	159	1500	ML/FL
OC2	25	40	6000	FL
OC3	50	159	3000	ML/FL
OC4	100	637	1500	ML
OC5	100	159	6000	FL

Figure 4 establishes the main differences among the three FC studied and their influence on the efficiency calculation procedure when there is no shifting profile. This allows to assess the effect of the FC on the instantaneous power losses factor (IPL factor).
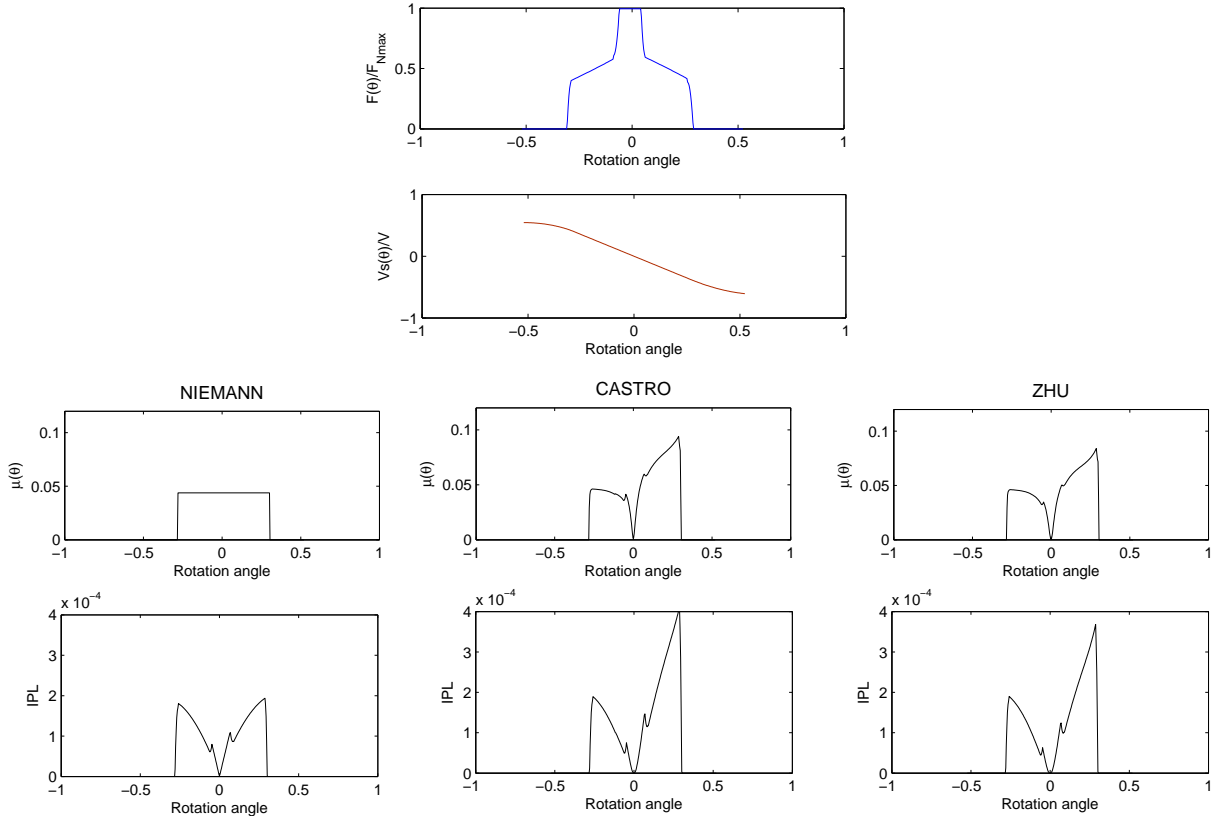

Fig. 4: Comparison among factors, on which efficiency depends, for the three FC formulations (159 Nm and 1500 rpm)

As commented, to calculate the load sharing (LS) by the LCM in quasi-static regime, the friction forces were considered to reach the equilibrium. Since the FC formulations were different, variations of the load sharing in the single contact region were expected in each case (Figure 3). As these variations among LS cases were slight, only the LS corresponding to Castro *et al.* is presented during the study, for the sake of simplicity.

Regarding the FC formulations, both hybrid formulations have their highest value at the end of the second double-contact region. This fact and the sliding velocity reaching its maximum value in the same region result in the highest magnitude of IPL factor. Thus, with no shifting, it is expected that efficiency corresponding to both hybrid formulations reaches lower values than those calculated with Niemann's FC, and what is more, as Castro FC has a higher maximum than the Zhu FC, it is envisaged that the former reaches the lowest efficiency of the three studied FC.

Once the no shifting case was analysed, the strategy to assess the effect of the shifting profile in the efficiency is presented. Three cases of study were considered to evaluate the effect of shifting profile on the friction coefficient and, therefore, on the efficiency, in five operating conditions. The structure of the study is the same as in previous works [10], since the new results are compared with those obtained beforehand. Although the methodology to include the shifting was presented [10], a summary of this methodology is shown in order to aid the comprehension of the reader. In the first case of study, the contact length and location were fixed. The goal was to analyse the shifting effect in an isolated manner. Since a small range of shifting was assessed in this first case (mesh interference appeared with large shift factors), a second case study was performed, where the contact length was fixed whilst the location of the contact segment was varied. In this way, a new unknown was added to the effect of the shifting, the contact location impact. In the third case study, both the contact location and length were varied. So as to help the understanding of the case studies layout, the assessment aim of each is presented in Table 4 and Figure 5.

Table 4: Case studies description summary

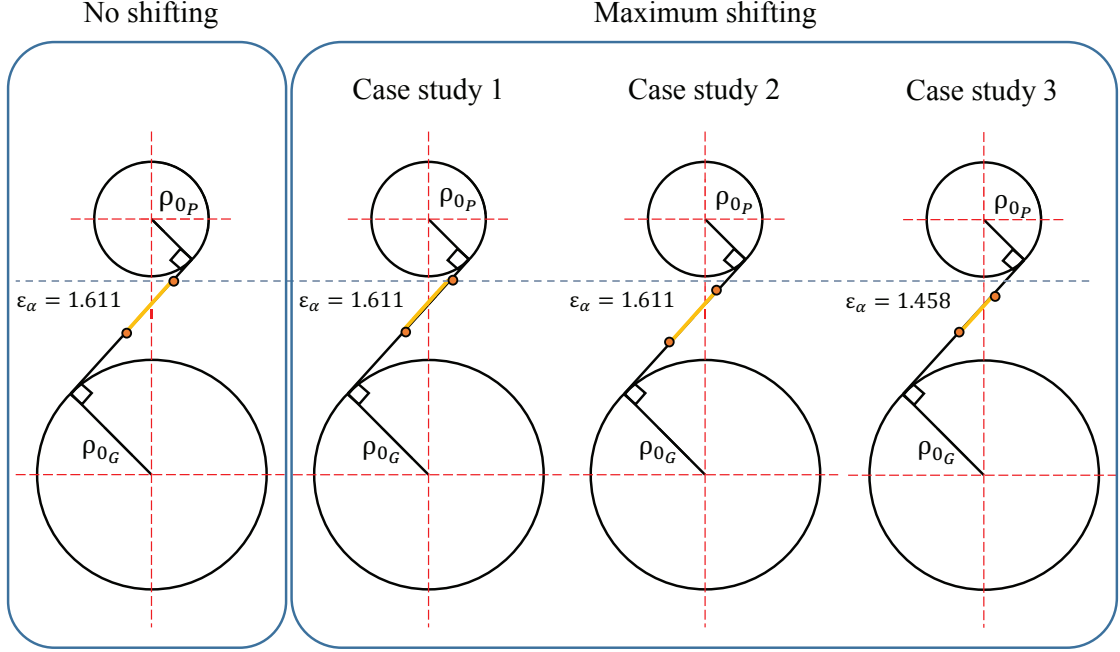| Case study Number	Contact length variation	Contact location variation
1	No	No
2	No	Yes
3	Yes	Yes

Fig. 5: Length and location of the contact segment in the extreme shifting factors of each case study

As appreciated, the level of complexity increases with each case study considered, isolating, in the first, the shifting effect on the FC, in the second, adding the change of contact segment location and, in the third, the variation of the segment length.

The methodology to calculate the exterior radii of the shifting case studies was also established in [10]. This is the reason why only a brief summary of the procedure of exterior radii calculation in each case of study is given next, for the sake of clarity.

In the first, the exterior radii of both pinion and driven gear were fixed to the case of null-shifting. The main consequence of this constraint is that the sliding velocity remains constant for all the shifting cases.

In the second case study, first, the contact ratio (ϵ_α) of the case study must be chosen, in this case was 1.611 (null-shift factor case). The, the tip contact ratio of the pinion (ε_1) was obtained by means of its exterior radius (R_{1ext}):

$$\varepsilon_1 = \frac{\sqrt{R_{1ext}^2 - (R_1\cos(\varphi))^2} - R_1\sin(\varphi)}{\pi m \cos(\varphi)} \rightarrow R_{1ext} = m(\frac{z_1}{2} + x_1 + dd_{hta}) \tag{11}$$

Lastly, the driven gear exterior radius (R_{2ext}) was calculated by its tip contact ratio (ε_2):

$$R_{2ext} = \sqrt{(R_2\sin(\varphi) + \varepsilon_2\pi m \cos(\varphi))^2 + (R_2\cos(\varphi))^2} \rightarrow \varepsilon_2 = \varepsilon_\alpha - \varepsilon_1 \tag{12}$$

In the third case study, the radii of the gears varied with the shift factor as detailed in equation 13.

$$\left.\begin{array}{l} R_{1ext} = m(\frac{z_1}{2} + x_1 + dd_{hta}) \\ R_{2ext} = m(\frac{z_2}{2} + x_2 + dd_{hta}) \end{array}\right\} \rightarrow \text{ where } x_2 = -x_1 \tag{13}$$

5 Results and Discussion

An efficiency assessment of shifted gear transmissions was performed in each shifting case study, using the LCM and three FC specified in the previous sections.

5.1 FIRST CASE STUDY: FIX EXTERIOR RADIUS

In Figure 6, the efficiency is shown for five operating conditions and a specific range of shift factor ($x_1\epsilon$[-0.05,0.2]).
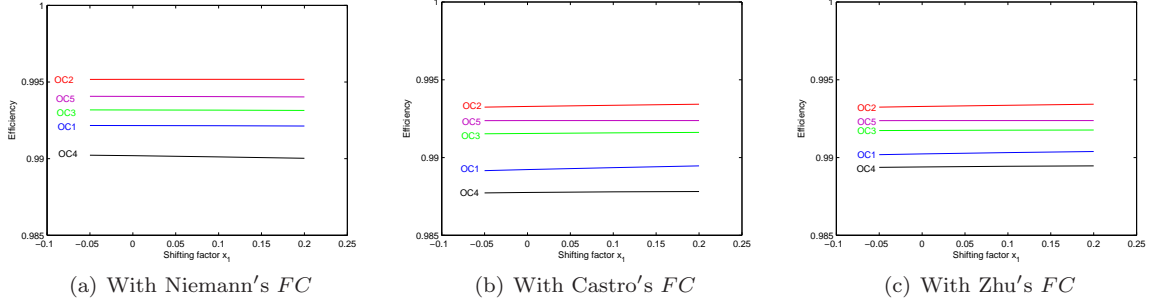

(a) With Niemann′s FC (b) With Castro′s FC (c) With Zhu′s FC

Fig. 6: Efficiency values when Niemann′s, Castro′s and Zhu′s friction coefficients were implemented (first case study)

From Figure 6, slight variations on the efficiency under the same operating conditions were observed. Nevertheless, for the three FC cases, the higher the torque ($OC4$), the lower the efficiency was, obtaining the trend when the speed decreased ($OC1$, $OC3$ and $OC5$).

Comparing the efficiency using the three FC formulations, Castro formulation presented the lowest efficiency values, being the ones corresponding to Niemann′s formulation the highest. It can be inferred that the FC formulation influences on the efficiency.

The parameters which affect the efficiency were evaluated individually. Henceforth, despite the fact that a comparison considering all the operating conditions is performed, only $OC1$, $OC2$ and $OC4$ will be shown in the figures. $OC2$ and $OC4$ are the extreme levels of torque considered and $OC1$ presents significative deviations on the efficiency among FC formulations. Moreover, as shown in Figure 2, $OC1$ and $OC4$ were under mixed lubrication conditions, whilst $OC2$ was under fluid film lubrication conditions. Hence, a good representation of the two conditions of lubrication in EHL is obtained with these three operating conditions.

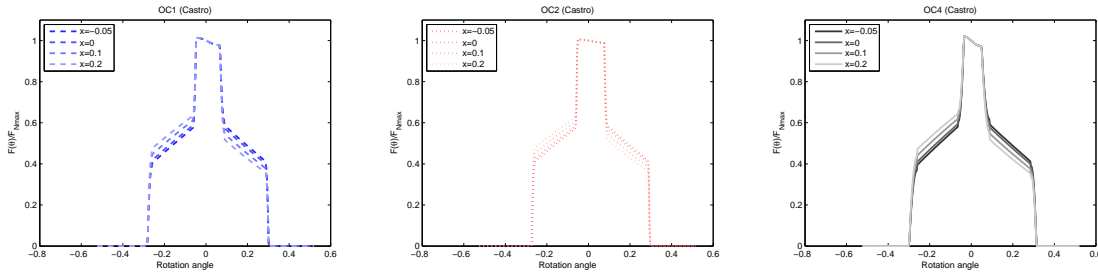The influence of the shifting on the load sharing is shown in Figure 7.

Fig. 7: LS when Castro′s FC was implemented in $OC1$, $OC2$ and $OC4$

If the effect of the shift coefficient on the LS is assessed, the higher the shifting, the higher the transmitted load is in the first double-contact region, as well as the lower the load is in the second double-contact region. Nevertheless, there was no difference among shifting cases in the single-contact region. Moreover, the contact ratio increased with the torque increment, thus, the single-contact length was getting shorter.

As appreciated in Figure 8, the effect of the shifting on the LS has no influence on the friction coefficient, since remained unchanged. Thus, the conclusions extracted, when there was no shifting, keeps fulfilling.
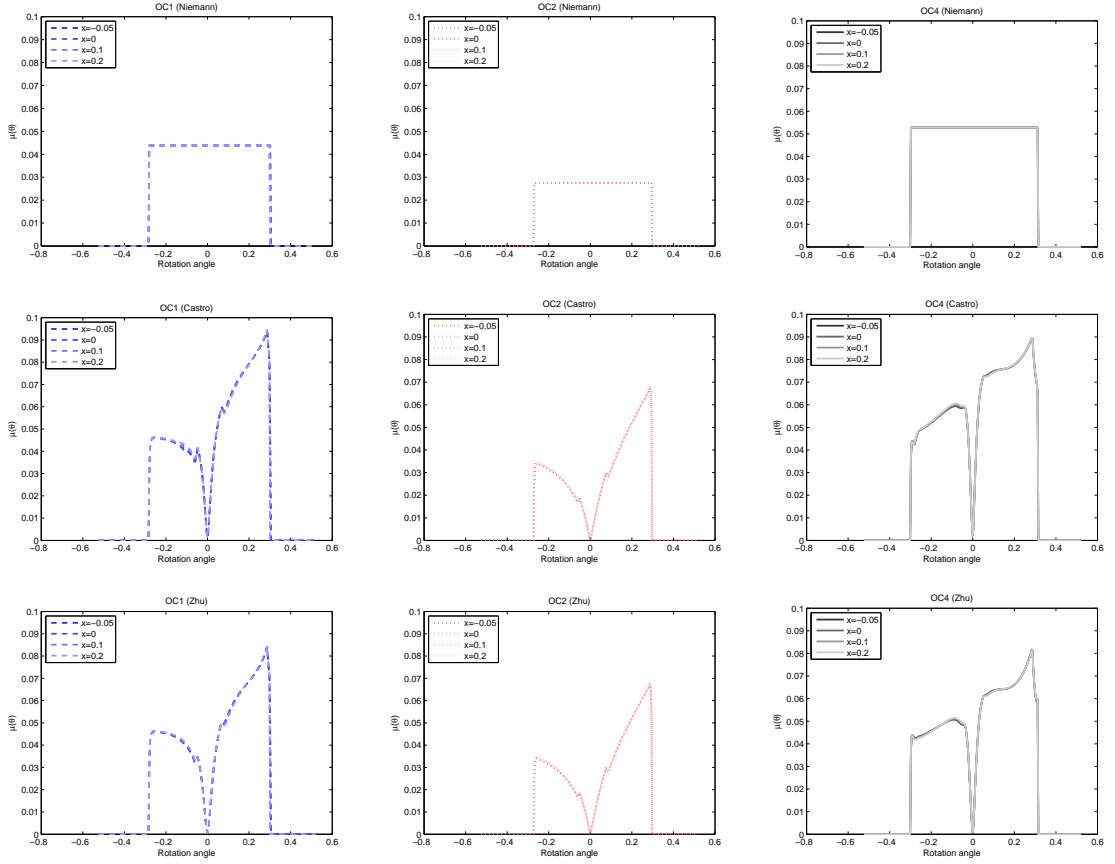

Fig. 8: FC for some shift factors in $OC1$, $OC2$ and $OC4$

Regarding the hybrid formulations, at the beginning and end of the contact, Castro and Zhu FCs reached their highest magnitude of FC, which also coincided with the maximum sliding velocity. Comparing between both formulations, they are similar in the first double-contact region and in the single-contact one, finding a distortion in the second double-contact region, where the Castro FC value is higher.

As stated before, in this case study, shifting did not affect Niemann's FC and only had slight effects on the hybrid formulations. For this reason, in Table 5, the FC mean values have been shown just for the maximum shifting case (these FC mean values are also applicable to the no shifting case). From Table 5, the mean value of the Niemann's FC was lower than the other two formulations.

Table 5: FC mean values with maximum profile shifting

FC mean values($x_1 = 0.2$)	OC1	OC2	OC3	OC4	OC5
Niemann	0.044	0.027	0.038	0.053	0.033
Castro *et al.*	0.054	0.033	0.042	0.063	0.038
Zhu *et al.*	0.048	0.033	0.041	0.062	0.038

Next is evaluated the impact of both the LS and FC on the IPL factor (Figure 9).

From the previous analysis of the FC and LS, it was inferred that the latter was the parameter which affects the IPL factor, with the shifting variations. On the other side, the shifting influence on the efficiency is almost negligible, this happens because, when the shift factor increased, the increment of the power losses at the contact beginning was compensated by the power losses diminution at the end of the contact.

The IPL factor, in the first double-contact and single-contact region, was similar for the three FC formulations, being at the end of the contact where there was a dispersion. As the LS in this region was equal for the three FC formulations, the parameter which produced this IPL distortion was the FC.

Assessing the operating conditions, as a general rule, the higher the resistive torque, the more generated power losses occurred, fulfilling also when the speed was reduced. To clarify this statement, the IPL factors, for the three FC formulations and for the maximum and minimum shift factors, are presented in Figure 10.
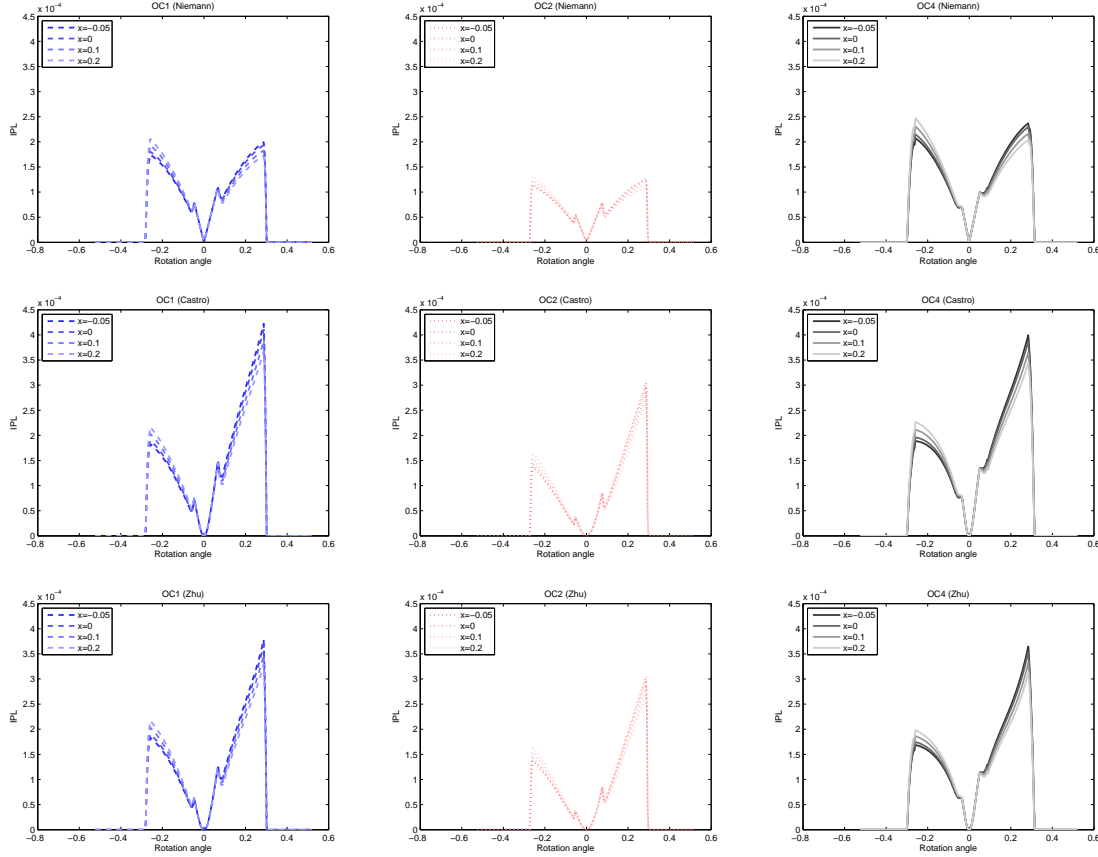
Fig. 9: IPL factors when the three FCs were used in $OC1$, $OC2$ and $OC4$

Furthermore, by means of this figure, it is also proven that the contact ratio (contact length) was higher with the torque increment, what turned into higher power losses.

These conclusions, regarding the operating conditions, remain for all the shifting case studies. Hence, although the figures are shown, no analysis is required in the subsequent cases of study.

5.2 SECOND CASE STUDY: FIXED THEORETICAL CONTACT RATIO

The efficiency values for the considered operating conditions and certain shift factors are presented in Figure 11. The range of shift factor was extended since mesh interference occurs with a larger value of this parameter in the first case study.

From Figure 11, it was observed that the efficiency variation with the shift coefficient had a similar tendency for the three FC formulations. There was a shift coefficient which made, under specific operating conditions, the efficiency optimal. In Niemann′s case, this value was close to 0.1 in the five operating conditions considered, nevertheless, in the other two FC formulations, this optimal shift value is dependent of the operating conditions considered. For instance, in $OC1$, $OC2$ and $OC4$, this shift value was approximately 0.2 in both hybrid formulations.

As in the previous case of study, the efficiency calculated using Niemann′s FC was the highest, followed by Zhu FC one, being the efficiency corresponding to Castro FC the lowest. Furthermore, regarding the
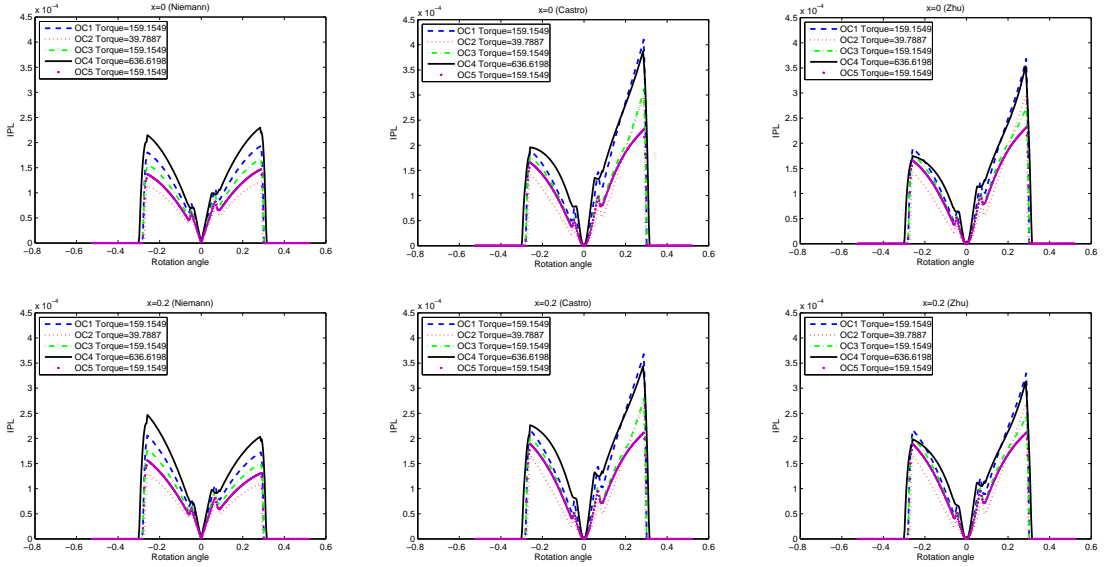
Fig. 10: IPL factors, when three FCs were implemented, in the extreme cases of profile shifting ($x_1 = 0$ and $x_1 = 0.2$)

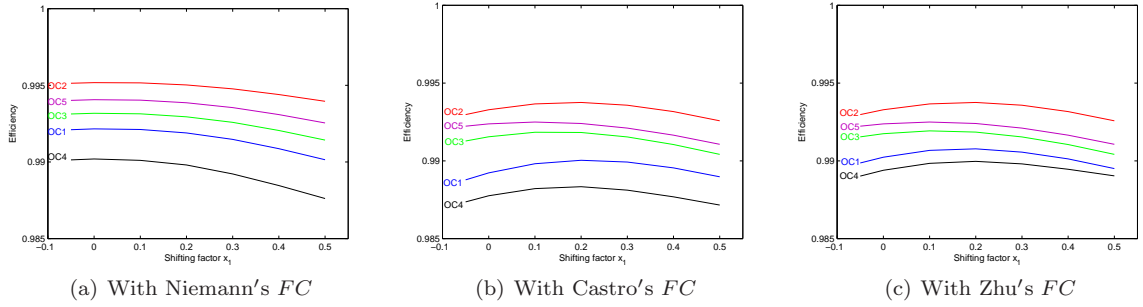(a) With Niemann's FC (b) With Castro's FC (c) With Zhu's FC

Fig. 11: Efficiency values when Niemann's, Castro's and Zhu's friction coefficients were implemented (second case study)

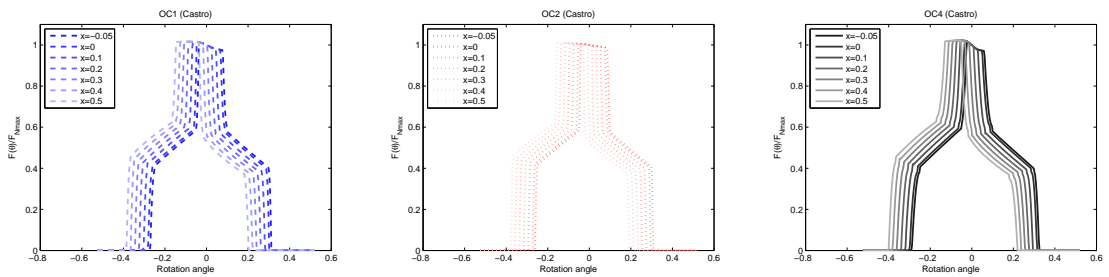Fig. 12: LS, when Castro's FC was used, in $OC1$, $OC2$ and $OC4$

operating conditions, what was exposed in the first case study remained, the efficiency was lower with the increment of torque level and the reduction of the speed.

To understand the tendency followed by the efficiency, the parameters, which affect it, were analysed. In Figure 12, the LS is shown for the three specified operating conditions and all the shifting cases.

The transmitted load was higher in the first double-contact region and lower in the second, with respect to the transmitted load when there was no shifting. Besides this LS modification, the shifting produced the change of the contact location, starting and finishing before with the shift factor increment.
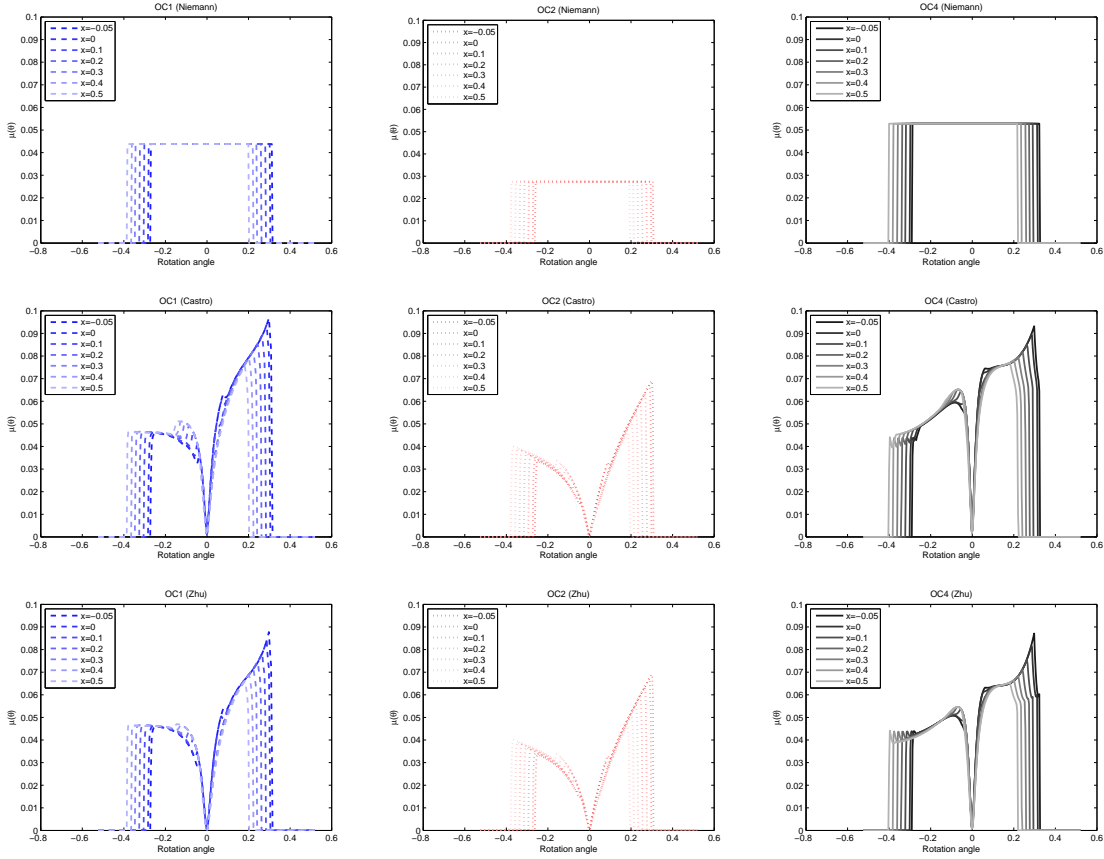
Fig. 13: FC for different shift factors in $OC1$, $OC2$ and $OC4$

As something remarkable, from a specific shift factor on (0.3-0.4 in this case study), the single-contact region occurred before the pitch point, thus, the FC effect on the LS single-contact region was palliated.

By means of Figure 13, the influence of the shift factor and operating conditions on FC was analysed. In order to aid the understanding of this figure, the FC mean values, with the maximum shift factor ($x_1 = 0.5$), were enclosed in Table 6.

Due to the shift coefficient, the contact started and ended before, as a matter of fact this had a major impact on the FC hybrid formulations, which had a lower value at the contact beginning than at the end. These facts turned into a diminution of the FC mean value with the increment of shifting, as shown in Table 6. In fact, the Niemann's mean value was lower than the others in the first case study (without shifting), nevertheless, this tendency changed with the maximum shift factor, where the three formulations had a similar mean value. Concluding that the shift factor produced a lessening in the mean value of the hybrid FC, whilst the Niemann's one was not affect.

To assess the operating conditions, the aid of the table was compulsory. It kept fulfilling that the FC mean value was higher, in all the formulations, with the increment of torque and the lessening of the speed.

Table 6: FC mean values with maximum profile shifting value

FC mean values($x_1 = 0.5$)	OC1	OC2	OC3	OC4	OC5
Niemann	0.044	0.027	0.038	0.053	0.033
Castro *et al.*	0.046	0.029	0.039	0.055	0.036
Zhu *et al.*	0.043	0.029	0.039	0.047	0.036

Both parameters (FC and LS) had an impact on the IPL factor (shown in Figure 14).

From the previous analysis of the FC and LS, the latter is parameter which affected the change in the IPL factor at the beginning of the contact, being both parameters decisive at the end of the contact. The first statement fulfils because the FC in this region was almost constant, in all the shifting cases, for

the three FC formulations, whilst LS was not. At the contact end, a diminishing of the power losses was observed, in Niemann's case due to the LS (FC was constant), whilst, in the hybrid formulations case, this reduction was greater mainly due to the FC decrease (LS is also reduced). This is the reason why there is a shift factor to which the efficiency increases. Thus, the friction coefficient formulation is decisive to find the shift factor which makes optimal the efficiency of the system.
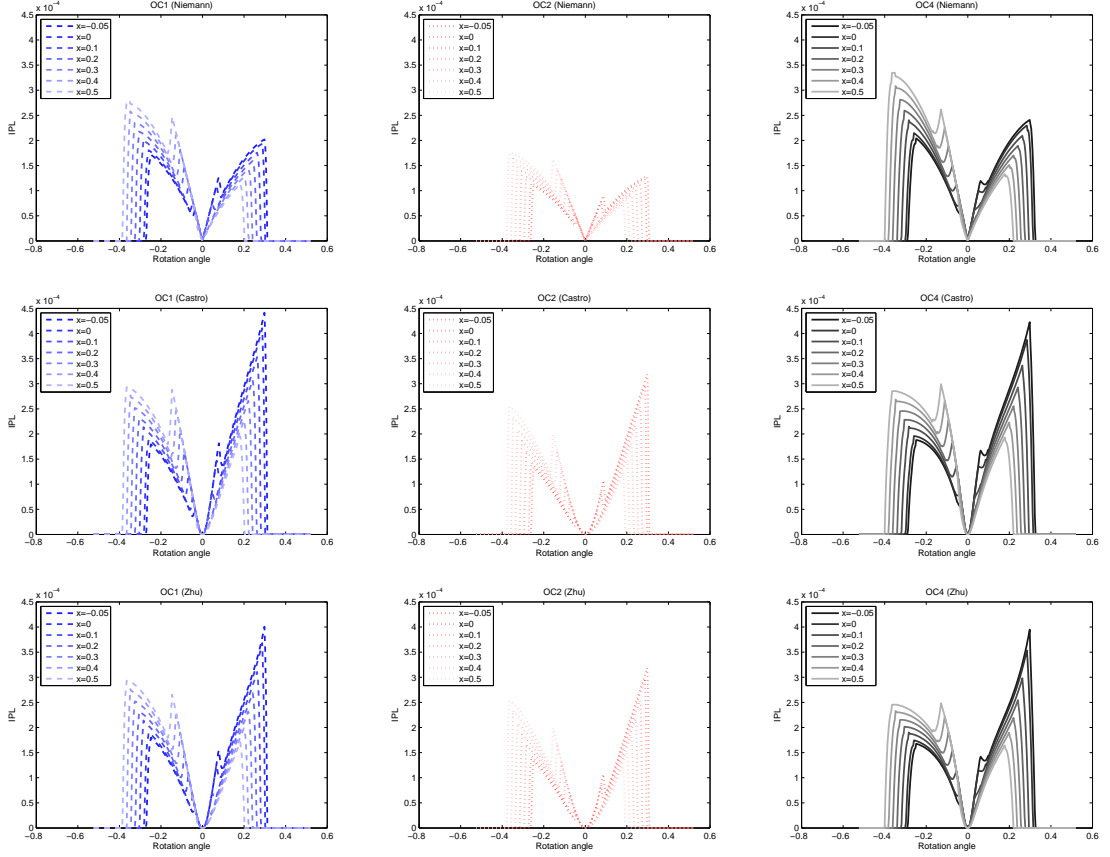

Fig. 14: IPL factors in $OC1$ $OC2$ and $OC4$ for several profile shifting cases

In Figure 15, IPL factors, for the extreme shift factor cases, using the three FC formulations are presented.

5.3 THIRD CASE STUDY: EXTERIOR RADII DEPEND ON THE SHIFT COEFFICIENT

In Figure 16, the efficiency of the system is shown, for the three considered FC formulations, in different shift factor cases and operating conditions.

Regarding the effect of the shifting on the efficiency, there was an optimal shift factor, which makes the efficiency maximum, dependant of the implemented FC formulation and operating conditions of the transmission.

To explain this efficiency tendency with the shifting, the parameters, on which efficiency depends, must be analysed. The first studied parameter was the LS, by means of Figure 17.

As in the previous case studies, the shift factor produced that the transmitted load, in the first and second double-contact regions, was different with respect to the null-shift case. Nevertheless, with the shifting increment, the LS location was also modified, "moving" to the left, as well as its contact length was shortened. These facts affected the FC (18).

The length shortening and location change of the contact, due to the shift factor increment, had an important impact on the FC, since the two hybrid formulations had a lower FC value at the beginning than at the end. Thus, when the shift factor increased, the FC kept approximately constant at the beginning of
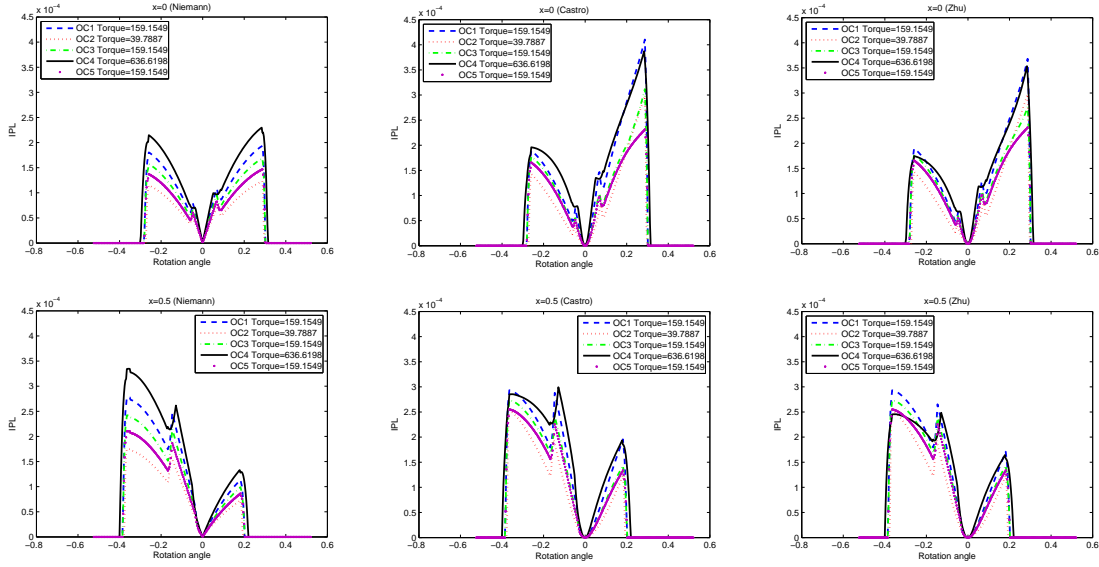
Fig. 15: IPL factors, when the three FCs were implemented, in the extreme cases of profile shifting ($x_1 = 0$ and $x_1 = 0.5$)

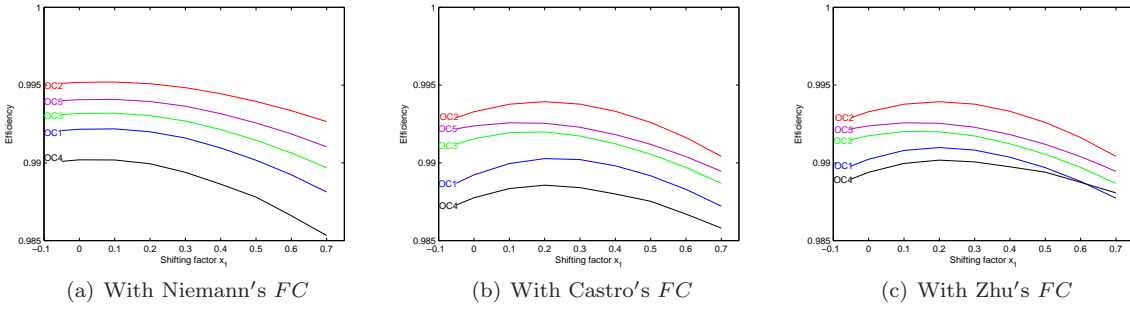(a) With Niemann's FC (b) With Castro's FC (c) With Zhu's FC

Fig. 16: Efficiency values when Niemann's, Castro's and Zhu's friction coefficients were implemented (third case study)
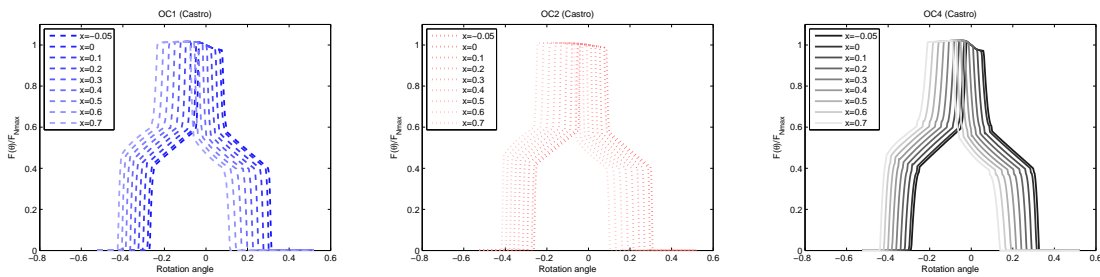

Fig. 17: LS when Castro's FC was used ($OC1$, $OC2$ and $OC4$)

the contact, getting sharply lower at the end. This is perfectly observed by the FC mean values, as they were lower, in the maximum shift factor case, than in the null-shifting one (Table 7).

Both the LS and the FC affected the power losses, as presented in Figure 19.

With the shifting increment, there was a power losses increase at the contact beginning, existing a power losses reduction at the end. From the previous analysis of the LS and FC, the former is the parameter which affected the increment of the IPL factor, at the beginning of the contact, because this factor was similar for the three FC formulations. Nevertheless, both parameters (LS and FC) are determinant of the power losses
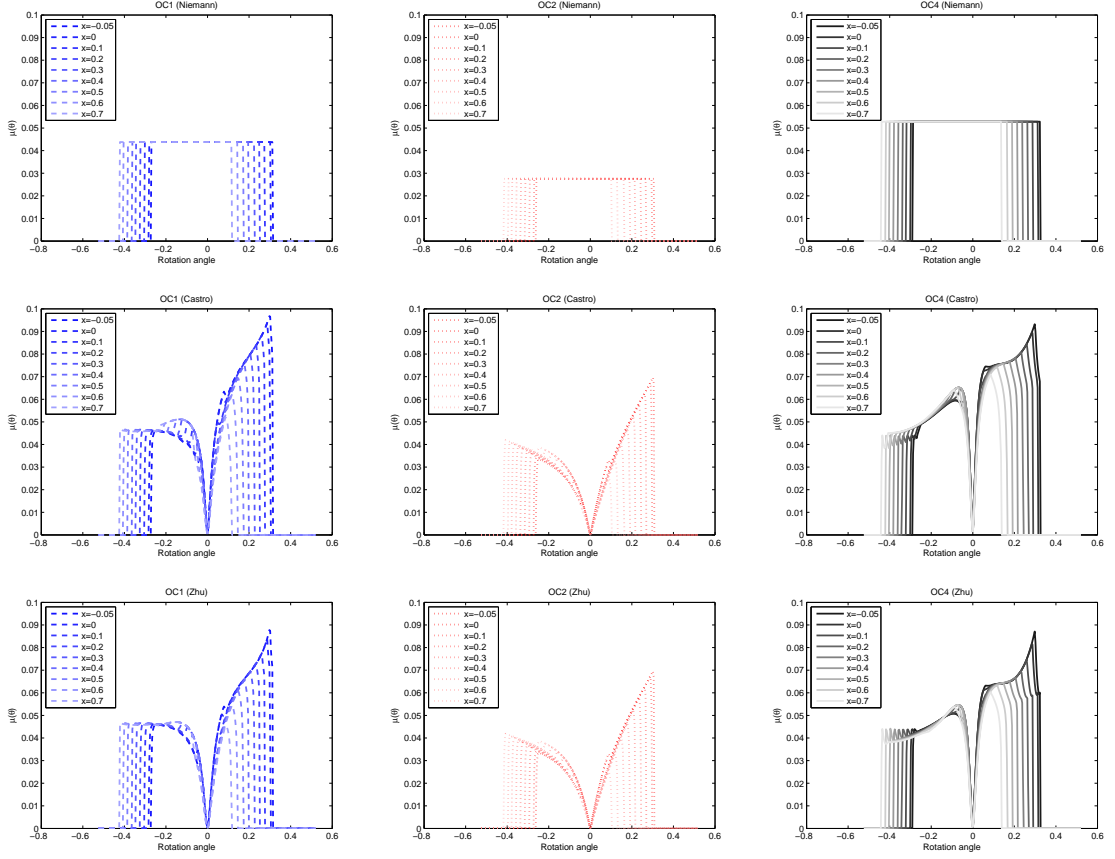
Fig. 18: FC in $OC1$ $OC2$ and $OC4$ for several shift factors

Table 7: FC mean values with maximum profile shifting value

FC mean values($x_1 = 0.7$)	OC1	OC2	OC3	OC4	OC5
Niemann	0.044	0.027	0.038	0.053	0.033
Castro _et al._	0.041	0.028	0.035	0.050	0.033
Zhu _et al._	0.039	0.028	0.036	0.042	0.033

reduction, at the contact end, and their importance depended on the implemented FC formulation. Whilst, in Niemann's case, the power losses reduction occurred due to the LS since the FC kept constant, in the hybrid formulations, this reduction was sharper and due to the fact that both the FC and LS diminished in this region. Explaining, in this way, why the efficiency increased for small values of shifting and then decreased.

The IPL factors, in extreme shift factors ($x_1 = 0$ and $x_1 = 0.7$), were shown for the three FC formulations (Figure 20).

6 Conclusions

The effect of the friction coefficient choice on the efficiency of shifted spur gears was analysed in this study. This is of great interest in order to evaluate the benefit of incorporating an enhanced friction coefficient to the efficiency calculation compared with traditional approaches, which generally uses constant friction coefficient formulations.

In this proposal, the friction was implemented by using three friction coefficient formulations, the well-known Niemann's and two hybrid formulations derived from the Xu _et al._. The efficiency results obtained implementing the hybrid formulations were compared with those calculated including Niemann's friction coefficient, showing the improvement of using an enhanced friction coefficient in the efficiency calculation.
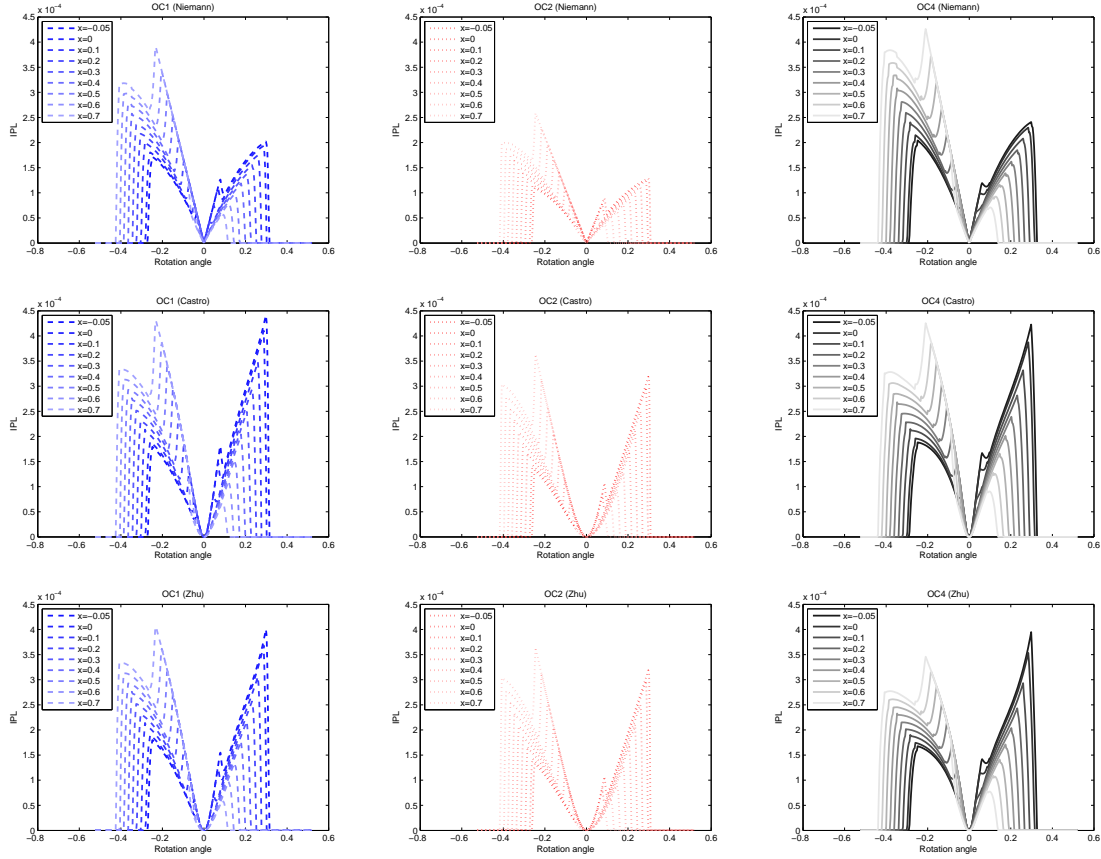
Fig. 19: IPL factor when the three FCs were implemented in $OC1$ $OC2$ and $OC4$
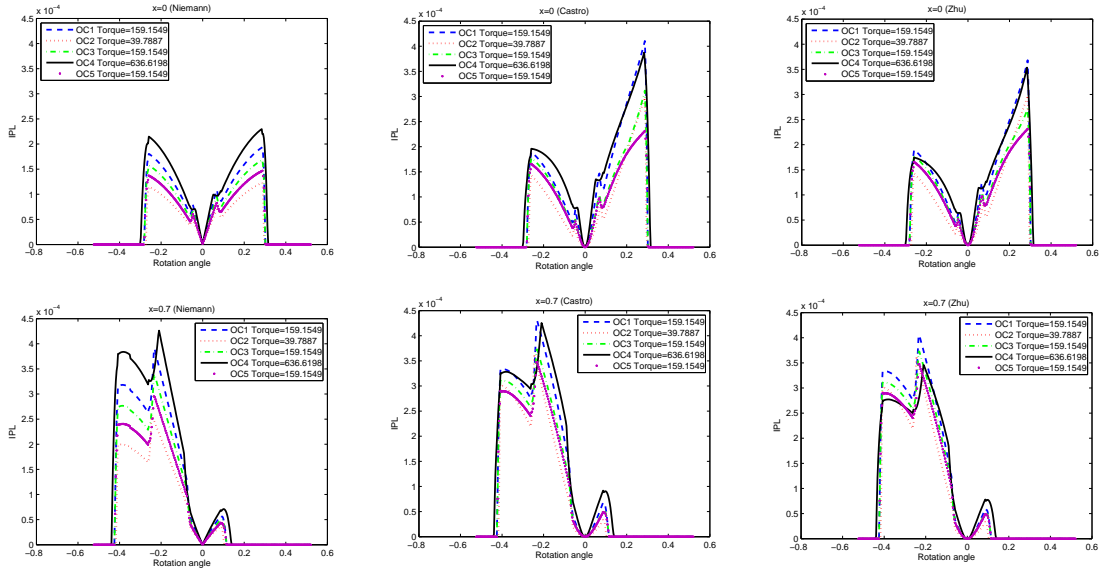

Fig. 20: IPL factors, when the three FCs were employed, in the extreme cases of profile shifting ($x_1 = 0$ and $x_1 = 0.7$)

In this work, it was appreciated that friction coefficient formulation choice affected substantially the efficiency, obtaining lower values of this parameter when the hybrid formulations were included than those calculated using Niemann′s formulation. Moreover, the three formulations were susceptible to change with

the operating conditions variation, as a matter of fact, they reacted in a similar way when the torque or speed changed. Specifically, the higher the torque and the lower the speed, the higher the mean friction coefficient was and therefore, the lower the efficiency value was.

One outcome from the efficiency calculation was that there was a shift factor which made it optimal. Although the operating conditions affected this value, it mainly depended on the friction coefficient formulation implemented.

As a matter of interest, the use of shifting in spur gears produced a decrease in the friction coefficient mean value due to the contact location variation. Even though it could be thought that this fact led to an efficiency increment, this statement was not always true. Specifically, as the single contact did not take place on the pitch point region anymore, as well as the load and sliding velocity became higher at the contact beginning, an overall power losses increment was produced with the shift factor increment. Thus, a reduction of the friction coefficient mean value with the shifting could led to an efficiency lessening.

Although an accurate friction coefficient simulate better the behaviour of the frictional effects, the use of a constant friction coefficient provide a similar efficiency value. Thus, depending on the application, the use of a constant friction coefficient might be justified instead of an enhanced formulation. For instance, in a preliminary phase of standard gear transmission design, the use of a constant friction coefficient is generally acceptable, whilst in a multistage transmission such as planetary gear sets, as there are several contacts simultaneously, this assumption would lead to an important error in the system efficiency.

References

1. F. Ali, I. Křupka, and M. Hartl. Analytical and experimental investigation on friction of non-conformal point contacts under starved lubrication. *Meccanica*, 48(3):545–553, 2013.
2. N. E. Anderson and S. H. Loewenthal. Effect of geometry and operating conditions on spur gear system power loss. *Journal of mechanical design*, 103(4):151–159, 1981.
3. S. Baglioni, F. Cianetti, and L. Landi. Influence of the addendum modification on spur gear efficiency. *Mechanism and Machine Theory*, 49:216–233, 2012.
4. J.A. Brandão, M. Meheux, F. Ville, J. Seabra, and J. Castro. Comparative overview of five gear oils in mixed and boundary film lubrication. *Tribology International*, 47:50–61, 2012.
5. J. Castro and J. Seabra. Coefficient of friction in mixed film lubrication: Gears versus twin-discs. *Proceedings of the Institution of Mechanical Engineers, Part J: Journal of Engineering Tribology*, 221(3):399–411, 2007.
6. F. Chaari, M.S. Abbes, F.V. Rueda, A.F. del Rincon, and M. Haddar. Analysis of planetary gear transmission in non-stationary operations. *Frontiers of Mechanical Engineering*, 8(1):88–94, 2013.
7. W. Chong and M. De La Cruz. Elastoplastic contact of rough surfaces: A line contact model for boundary regime of lubrication. *Meccanica*, 49(5):1177–1191, 2014.
8. M. De La Cruz, W. Chong, M. Teodorescu, S. Theodossiades, and H. Rahnejat. Transient mixed thermo-elastohydrodynamic lubrication in multi-speed transmissions. *Tribology International*, 49:17–29, 2012.
9. A. Diez-Ibarbia, A.F. del Rincón, M. Iglesias, A. De Juan, P. García, and F. Viadero. Efficiency analysis of shifted spur gear transmissions. *Mechanisms and Machine Science*, 24:373–381, 2015.
10. A. Diez-Ibarbia, A.F. del Rincon, M. Iglesias, A. de Juan, P. Garcia, and F. Viadero. Efficiency analysis of spur gears with a shifting profile. *Meccanica*, 51(3):707–723, 2016.
11. V. Elisaus, M. Mohammadpour, S. Theodossiades, and H. Rahnejat. Effect of teeth micro-geometrical form modification on contact kinematics and efficiency of high performance transmissions. *Proceedings of the Institution of Mechanical Engineers, Part K: Journal of Multi-body Dynamics*, 0(0):1–18, 2017.
12. C.R. Evans and University of Cambridge. *Measurement and Mapping of the Rheological Properties of Elastohydrodynamic Lubricants*. University of Cambridge, 1983.
13. Z. Feng, S. Wang, T.C. Lim, and T. Peng. Enhanced friction model for high-speed right-angle gear dynamics. *Journal of Mechanical Science and Technology*, 25(11):2741–2753, 2011.
14. C. Fernandes, P. Marques, R. Martins, and J. Seabra. Gearbox power loss. part ii: Friction losses in gears. *Tribology International*, 88:309 – 316, 2015.
15. A. Fernández del Rincón, M. Iglesias, A. De-Juan, P. García, R. Sancibrián, and F. Viadero. Gear transmission dynamic: Effects of tooth profile deviations and support flexibility. *Applied Acoustics*, 77(0):138–149, 3 2014.
16. A. Fernández del Rincón, F. Viadero, M. Iglesias, A. De-Juan, P. García, and R. Sancibrian. Effect of cracks and pitting defects on gear meshing. *Proc IMechE Part C: J Mechanical Engineering Science*, 226(11):2805–2815, 2012.
17. A. Fernández Del Rincón, F. Viadero, M. Iglesias, P. García, A. De-Juan, and R. Sancibrian. A model for the study of meshing stiffness in spur gear transmissions. *Mechanism and Machine Theory*, 61:30–58, 2013.
18. B. J. Hamrock, S.R. Schmid, and B.O. Jacobson. *Fundamentals of Fluid Film Lubrication*. New York: Marcel Dekker, second edition edition, 2004.
19. B. R Höhn. Improvements on noise reduction and efficiency of gears. *Meccanica*, 45(3):425–437, 2010.
20. M. Iglesias, A. Fernandez del Rincon, A. de Juan, P. Garcia, A. Diez-Ibarbia, and F. Viadero. Planetary transmission load sharing: Manufacturing errors and system configuration study. *Mechanism and Machine Theory*, 111:21–38, 2017.
21. J. Kuria and J. Kihiu. Prediction of overall efficiency in multistage gear trains. *World Academy of Science, Engineering and Technology*, 74:50–56, 2011.
22. S. Li and A. Kahraman. Prediction of spur gear mechanical power losses using a transient elastohydrodynamic lubrication model. *Tribology Transactions*, 53(4):554–563, 2010.

23. H. Ma, M. Feng, Z. Li, R. Feng, and B. Wen. Time-varying mesh characteristics of a spur gear pair considering the tip-fillet and friction. *Meccanica*, pages 1–15, 2016.

24. K. F. Martin. A review of friction predictions in gear teeth. *Wear*, 49(2):201–238, 1978.

25. R. Martins, J. Seabra, A. Brito, Ch. Seyfert, R. Luther, and A. Igartua. Friction coefficient in fzg gears lubricated with industrial gear oils: Biodegradable ester vs. mineral oil. *Tribology International*, 39(6):512–521, 2006.

26. K. Michaelis, B. R Höhn, and M. Hinterstoißer. Influence factors on gearbox power loss. *Industrial Lubrication and Tribology*, 63(1):46–55, 2011.

27. M. Mohammadpour, S. Theodossiades, and H. Rahnejat. Multiphysics investigations on the dynamics of differential hypoid gears. *Journal of Vibration and Acoustics, Transactions of the ASME*, 136(4), 2014.

28. M. Mohammadpour, S. Theodossiades, and H. Rahnejat. Transient mixed non-newtonian thermo-elastohydrodynamics of vehicle differential hypoid gears with starved partial counter-flow inlet boundary. *Proceedings of the Institution of Mechanical Engineers, Part J: Journal of Engineering Tribology*, 228(10):1159–1173, 2014.

29. M. Mohammadpour, S. Theodossiades, H. Rahnejat, and T. Saunders. Non-newtonian mixed elastohydrodynamics of differential hypoid gears at high loads. *Meccanica*, 49(5):1115–1138, 2014.

30. E. Mucchi, A. Rivola, and G. Dalpiaz. Modelling dynamic behaviour and noise generation in gear pumps: Procedure and validation. *Applied Acoustics*, 77:99–111, 2014.

31. Official Journal of the European Communities. *Commission regulation (EC) No 692/2008 of 18 July 2008 implementing and amending regulation (EC) No 715/2007 of the european parliament and of the council on type-approval of motor vehicles with respect to emissions from light passenger and commercial vehicles (euro 5 and euro 6) and on access to vehicle repair and maintenance information (1)*. Official Journal of the European Communities, 2008.

32. H. Ohlendorf. Verlustleistung und erwärmung von stirnrädern, 1958.

33. L. Paouris, R. Rahmani, S. Theodossiades, H. Rahnejat, G. Hunt, and W. Barton. An analytical approach for prediction of elastohydrodynamic friction with inlet shear heating and starvation. *Tribology Letters*, 64(1), 2016.

34. T. T. Petry-Johnson, A. Kahraman, N. E. Anderson, and D. R. Chase. An experimental investigation of spur gear efficiency. *Journal of Mechanical Design, Transactions of the ASME*, 130(6):0626011–06260110, 2008.

35. M. B. Sánchez, J. I. Pedrero, and M. Pleguezuelos. Critical stress and load conditions for bending calculations of involute spur and helical gears. *International Journal of Fatigue*, 48:28–38, 2013.

36. M. B. Sánchez, M. Pleguezuelos, and J. I. Pedrero. Enhanced model of load distribution along the line of contact for non-standard involute external gears. *Meccanica*, pages 1–17, 2012.

37. L. Vedmar and B. Henriksson. A general approach for determining dynamic forces in spur gears. *Journal of Mechanical Design, Transactions of the ASME*, 120(4):593–598, 1998.

38. F. Viadero, A. Fernández, M. Iglesias, A. De-Juan, E. Liaño, and M.A. Serna. Non-stationary dynamic analysis of a wind turbine power drivetrain: Offshore considerations. *Applied Acoustics*, 77:204–211, 2014.

39. F. Viadero, A. Fernandez Del Rincon, R. Sancibrian, P. Garcia Fernandez, and A. De Juan. A model of spur gears supported by ball bearings. In *WIT Transactions on Modelling and Simulation*, volume 46, pages 711–722, 2007.

40. H. Xu. Development of a generalized mechanical efficiency prediction methodology for gear pairs, 2005.

41. H. Xu. A novel formula for instantaneous coefficients of sliding friction in gearing. *SAE Technical Papers*, 2007.

42. T. Yada. Review of gear efficiency equation and force treatment. *JSME International Journal, Series C: Dynamics, Control, Robotics, Design and Manufacturing*, 40(1):1–8, 1997.

43. D. Zhu and Y.Z. Hu. A computer program package for the prediction of ehl and mixed lubrication characteristics, friction, subsurface stresses and flash temperatures based on measured 3-d surface roughness. *Tribology Transactions*, 44(3):383–390, 2001.